Pramana – J. Phys. (2017) 88: 43
DOI 10.1007/s12043-016-1328-1

Alpha decay and cluster decay of some neutron-rich actinide nuclei

G M CARMEL VIGILA BAI[1] and R NITHYA AGNES[2,*]

[1]Department of Physics, Rani Anna Government College for Women, Tirunelveli 627 008, India
[2]Department of Physics, St. John's College, Palayamkottai 627 002, India
*Corresponding author. E-mail: rcalvinsamuel@gmail.com

MS received 18 July 2015; revised 1 June 2016; accepted 20 July 2016; published online 9 February 2017

Abstract. Nuclei in the actinide region are good in exhibiting cluster radioactivity. In the present work, the half-lives of α-decay and heavy cluster emission from certain actinide nuclei have been calculated using cubic plus Yukawa plus exponential model (CYEM). Our model has a cubic potential for the overlapping region which is smoothly connected by a Yukawa plus exponential potential for the region after separation. The computed half-lives are compared with those of other theoretical models and are found to be in good agreement with each other. In this work, we have also studied the deformation effects on half-lives of cluster decay. These deformation effects lower the half-life values and it is also found that the neutron-rich parent nuclei slow down the cluster decay process. Geiger–Nuttal plots for various clusters are found to be linear and most of the emitted clusters are α-like nuclei.

Keywords. Alpha decay; cluster radioactivity; spontaneous fission.

PACS Nos 23.60.+e; 23.70.+j

1. Introduction

The process of spontaneous emission of fragments heavier than α-particles but lighter than the lightest fission fragment is known as cluster radioactivity. Theoretically, such emissions were first predicted by Sandulescu *et al* [1]. The first experimental observation was made by Rose and Jones [2]. Two types of models exist in explaining the exotic decay process. One is the preformed cluster model [3–5], in which the cluster is assumed to be preborn in a parent nucleus before it penetrates the barrier. Another is the fission model [6–8], in which the nucleus deforms continuously as it penetrates the nuclear interacting barrier and reaches scission configuration after running down the Coulomb barrier.

Many theoretical models were developed to study the cluster radioactivity. The role of deformation effect on half-lives in cluster decay has been studied by many researchers using different theoretical models [9–12]. In this paper, we have calculated the half-life of all the possible cluster emissions from the neutron-rich actinide parent nuclei by including quadrupole and hexadecapole deformations of the decaying parent nucleus along with that of the mitted cluster and daughter nucleus using cubic plus Yukawa plus exponential model (CYEM). This region is a fertile region in exhibiting cluster radioactivity because most of the daughter nuclei are the double magic nuclei or a neighbouring nucleus. In this model, the zero-point vibration energy is explicitly used without violating the energy conservation and the inertial mass coefficient dependent on the centre of mass distance. In §2 we have done our calculations by considering Coulomb plus Yukawa plus exponential potential as the interacting barrier for separated fragments and the cubic potential for the overlap region. The results and discussions are given in §3. Finally, the conclusions from our study are given in §4.

2. Cubic plus Yukawa plus exponential model

In this work, the parent and the emitted cluster are considered to be spheroid, keeping the daughter as spherical. If the emitted cluster has a deformation, say quadrupole deformation only while the daughter nuclear is spherical and if the Q-value of the reaction is taken as the origin, the potential for the post-scission

Table 1. Comparison of calculated values of logarithmic half-lives for α-decay of some actinide nuclei with deformation (WD) and without deformation (WOD).

Parent nuclei	Daughter nuclei		Emitted cluster		Q	log T (s)					Decay constant (s^{-1})
						Calculated		Reference			
	Z_d	A_d	Z_e	A_e	(MeV)	CYEM (WOD)	CYEM (WD)	ELDM [21]	Expt. [22]	ASAFM [23]	Calculated
$_{95}Am^{232}$	91	228	2	4	7.28	2.39	2.34	2.54	1.89	3.6	2.823×10^{-4}
$_{95}Am^{234}$	91	230	2	4	6.88	3.99	3.90	4.13	–	5.6	7.091×10^{-5}
$_{95}Am^{235}$	91	231	2	4	6.71	4.71	4.63	4.84	–	5.3	1.351×10^{-5}
$_{95}Am^{237}$	91	233	2	4	6.19	7.13	7.02	7.24	7.18	7.2	5.137×10^{-8}
$_{95}Am^{238}$	91	234	2	4	6.05	7.83	7.72	7.93	–	9.3	1.025×10^{-8}
$_{95}Am^{239}$	91	235	2	4	5.92	8.50	8.36	8.55	–	8.7	2.192×10^{-9}
$_{95}Am^{240}$	91	236	2	4	5.71	9.64	9.46	9.73	–	11.0	1.588×10^{-10}
$_{95}Am^{241}$	91	237	2	4	5.64	10.02	9.82	10.09	10.13	10.2	6.618×10^{-11}
$_{95}Am^{242}$	91	238	2	4	5.59	10.29	10.52	10.36	–	11.7	3.554×10^{-11}
$_{96}Cm^{238}$	94	234	2	4	6.62	6.53	6.40	5.64	3.94	4.9	2.045×10^{-7}
$_{96}Cm^{239}$	94	235	2	4	6.59	6.66	6.52	5.77	–	7.0	1.516×10^{-7}
$_{96}Cm^{240}$	94	236	2	4	6.40	7.55	7.35	6.63	6.37	6.5	1.953×10^{-8}
$_{96}Cm^{241}$	94	237	2	4	6.18	8.65	8.44	7.66	–	8.6	1.551×10^{-9}
$_{96}Cm^{242}$	94	238	2	4	6.22	8.42	8.19	7.49	7.15	7.2	2.635×10^{-9}
$_{96}Cm^{243}$	94	239	2	4	6.17	8.66	8.37	7.70	8.96	9.0	1.516×10^{-9}
$_{96}Cm^{244}$	94	240	2	4	5.90	10.10	9.80	9.08	8.76	8.8	5.506×10^{-11}
$_{96}Cm^{246}$	94	242	2	4	5.47	12.60	12.21	11.50	11.18	–	1.741×10^{-13}
$_{96}Cm^{248}$	94	244	2	4	5.16	14.59	14.11	13.46	13.04	–	1.781×10^{-15}
$_{96}Cm^{250}$	94	246	2	4	5.17	14.49	14.03	13.38	11.42	–	2.243×10^{-15}
$_{98}Cf^{248}$	96	244	2	4	6.36	8.61	8.20	7.63	7.46	–	1.701×10^{-9}
$_{98}Cf^{249}$	96	245	2	4	6.3	8.27	8.46	7.94	10.04	–	3.722×10^{-9}
$_{98}Cf^{250}$	96	246	2	4	6.13	9.78	9.26	8.77	8.62	8.6	1.150×10^{-10}
$_{98}Cf^{251}$	96	247	2	4	6.18	9.50	9.01	8.52	10.45	10.9	2.192×10^{-10}
$_{98}Cf^{252}$	96	248	2	4	6.22	9.27	8.74	8.28	7.92	8.0	3.722×10^{-10}
$_{98}Cf^{253}$	96	249	2	4	6.13	9.73	9.23	8.74	–	8.7	1.290×10^{-10}
$_{98}Cf^{254}$	96	250	2	4	5.93	10.81	10.26	9.79	–	9.3	1.073×10^{-11}
$_{98}Cf^{256}$	96	252	2	4	5.56	12.97	12.39	11.90	–	11.6	7.4256
$_{99}Es^{251}$	97	247	2	4	6.60	7.87	7.39	6.92	–	7.4	9.348×10^{-9}
$_{99}Es^{252}$	97	248	2	4	6.80	6.90	6.44	5.99	7.61	7.6	8.724×10^{-8}
$_{99}Es^{253}$	97	249	2	4	6.74	7.16	6.66	6.23	6.25	6.2	4.794×10^{-8}
$_{99}Es^{254}$	97	250	2	4	6.62	7.72	7.24	6.78	7.38	8.4	1.321×10^{-8}
$_{99}Es^{255}$	97	251	2	4	6.44	8.59	8.07	7.62	–	7.6	1.781×10^{-9}
$_{99}Es^{256}$	97	252	2	4	6.23	9.66	9.08	8.66	–	10.8	1.516×10^{-10}
$_{101}Md^{253}$	99	249	2	4	7.71	3.94	3.42	3.11	–	3.2	4.081×10^{-4}
$_{101}Md^{254}$	99	250	2	4	7.89	3.23	2.76	2.42	–	3.9	7.957×10^{-5}
$_{101}Md^{255}$	99	251	2	4	7.91	3.13	2.64	2.33	3.21	2.4	5.137×10^{-4}
$_{101}Md^{256}$	99	252	2	4	7.9	3.15	2.64	2.36	3.66	3.9	4.906×10^{-4}
$_{101}Md^{257}$	99	253	2	4	7.56	4.46	3.93	3.60	4.30	3.7	2.403×10^{-5}
$_{101}Md^{258}$	99	254	2	4	7.27	5.65	5.08	4.73	6.65	5.8	1.551×10^{-6}
$_{101}Md^{259}$	99	255	2	4	7.11	6.32	5.72	5.39	–	6.1	3.317×10^{-7}
$_{101}Md^{260}$	99	256	2	4	6.95	7.03	6.03	6.10	6.38	8.9	6.468×10^{-8}
$_{102}No^{250}$	100	246	2	4	8.96	0.03	−0.30	−0.65	−0.12	−1.2	0.6468
$_{102}No^{254}$	100	250	2	4	8.23	2.41	1.91	1.63	1.71	1.7	2.696×10^{-3}
$_{102}No^{255}$	100	251	2	4	8.44	1.65	1.18	0.88	2.27	2.8	1.50×10^{-2}
$_{102}No^{256}$	100	252	2	4	8.58	1.16	0.70	0.41	0.44	0.5	4.794×10^{-2}
$_{102}No^{257}$	100	253	2	4	8.45	1.58	1.09	0.81	–	2.1	1.823×10^{-2}

Table 1. *Continued.*

Parent nuclei	Daughter nuclei		Emitted cluster		Q	log T (s)					Decay constant (s^{-1})
						Calculated		Reference			
	Z_d	A_d	Z_e	A_e	(MeV)	CYEM (WOD)	CYEM (WD)	ELDM [21]	Expt. [22]	ASAFM [23]	Calculated
$_{102}No^{258}$	100	254	2	4	8.15	2.62	1.07	1.83	3.54	1.7	1.662×10^{-3}
$_{102}No^{259}$	100	255	2	4	7.88	3.61	2.09	2.77	–	4	1.701×10^{-4}
$_{102}No^{260}$	100	256	2	4	7.71	4.26	3.06	3.41	–	3.6	3.803×10^{-5}
$_{102}No^{262}$	100	258	2	4	7.31	5.87	3.64	4.97	–	6.1	9.348×10^{-7}

region as the function of the centre of mass distance r of the fragment is given by

$$V(r) = V_C(r) + V_n(r) - V_{df}(r) - Q. \quad (1)$$

Here V_C is the Coulomb potential between an emitted cluster and the spherical daughter. V_n is the nuclear interaction energy due to finite-range effects of Krappe *et al* and V_{df} is the change in nuclear interaction energy due to quadrupole deformation in the emitted cluster.

For a prolate spheroid emitted cluster with longer axis along the fission direction, Pik-Pichak [10] obtained

$$V_C(r) = \frac{3}{2}\frac{Z_d Z_e e^2 \gamma}{r}\left[\frac{1-\gamma^2}{2}\ln\frac{\gamma+1}{\gamma-1} + \gamma\right] \quad (2)$$

and for an oblate spheroid emitted cluster with shorter axis along the fission direction

$$V_C(r) = \frac{3}{2}\frac{Z_d Z_e e^2}{r}[\gamma(1+\gamma^2)\arctan\gamma^{-1} - \gamma^2]. \quad (3)$$

Here,

$$\gamma = \frac{r}{(a_e^2 - b_e^2)1/2},$$

Z_d, Z_e are the atomic numbers of the daughter and emitted cluster respectively, a_e and b_e are the semimajor and minor axes of the spheroidal cluster nucleus respectively.

For the overlapping region, we approximate the potential barrier by a third-order polynomial in r having the form (4)

$$V_C(r) = -E_v[V(r)_t + E_v]\left\{s_d\left(\frac{r-r_i}{r_t-r_i}\right)^2 - s_e\left(\frac{r-r_i}{r_t-r_i}\right)^3\right\}, \quad r_i \le r \le r_t, \quad (4)$$

where

$$r_t = a_e + R_d.$$

Here a_e is the semimajor (or) minor axis of the spheroid cluster depending on the prolate (or) oblate shape of the emitted cluster; and r_i is the distance between the centre of mass of the daughters and the emitted particle portions in the spheroid parent nucleus. The constants s_d and s_e appearing in eq. (4) are determined by requiring that the value of the potential $V(r)$ and its first derivative be continuous at the contact point $r = r_t$. Thus, we get

$$s_d = 3 - s \quad \text{and} \quad s_e = 2 - s,$$

where

$$s = \frac{r_t - r_i}{[V(r_t) + E_v]}\left[V_C'(r_t) + V_n'(r_t) - V_d'(r_t)\right]. \quad (5)$$

If the nuclei have spheroid shape, the radius vector $R(\theta)$ making an angle θ with the axis of symmetry locating sharp surface of a deformed nuclei is given by [13]

$$R(\theta) = R_0\left[1 + \sum_{n=0}^{\infty}\sum_{m=-n}^{n}\beta_{nm}Y_{nm}(\theta)\right]. \quad (6)$$

Here R_0 is the radius of the equivalent spherical nucleus.

If we consider spheroid deformation β_2, then

$$R(\theta) = R_0\left[1 + \beta_2\left(\frac{5}{4\pi}\right)^{1/2}\left(\frac{3}{2}\cos^2\theta - \frac{1}{2}\right)\right] \quad (7)$$

and if the Nilsson's hexadecapole deformation β_4 is also included in the deformation, then eq. (6) becomes

$$R(\theta) = R_0\left[1 + \beta_2\left(\frac{5}{4\pi}\right)^{1/2}\left(\frac{3}{2}\cos^2\theta - \frac{1}{2}\right) + \beta_4\left(\frac{9}{4\pi}\right)^{1/2}\frac{1}{8}(35\cos^4\theta - 30\cos^2\theta + 3)\right]. \quad (8)$$

Expressing the energies in MeV, lengths in fm and time in seconds, for calculating the lifetime of the decay system, we use the formula

$$T = \frac{1.433 \times 10^{-21}}{E_v}(1 + \exp(K)). \quad (9)$$

Table 2. Comparison of calculated values of logarithmic half-lives for cluster decays of some neutron-rich actinide nuclei with and without deformations.

Parent nuclei	Daughter nuclei	Emitted cluster	Q (MeV)	log T (s) Calculated CYEM (WOD)	Calculated CYEM (WD)	Reference ELDM [21]	Reference Expt. [24]	Reference ASAFM [23]	Branching ratio	Decay constant (s^{-1}) Calculated
$_{95}Am^{241}$	Tl^{209}	Si^{32}	90.66	29.52	28.49	26.59	–	28.9	18.29	2.093×10^{-30}
$_{95}Am^{241}$	Tl^{207}	Si^{34}	93.93	25.12	24.27	23.37	–	25.8	14.07	5.257×10^{-26}
$_{95}Am^{243}$	Tl^{209}	Si^{34}	90.77	29.82	28.55	27.25	–	29.9	17.15	1.049×10^{-30}
$_{96}Cm^{238}$	Pb^{206}	Si^{32}	97.26	22.22	21.44	20.45	–	21.8	17.32	4.1761×0^{-23}
$_{96}Cm^{239}$	Pb^{207}	Si^{32}	97.74	21.42	20.66	19.80	–	22.6	14.42	2.635×10^{-22}
$_{96}Cm^{240}$	Pb^{208}	Si^{32}	97.56	21.56	20.28	19.90	–	21.2	15.06	1.909×10^{-22}
$_{96}Cm^{240}$	Pb^{206}	Si^{34}	95.47	25.12	24.15	23.29	–	25.1	18.62	5.257×10^{-26}
$_{96}Cm^{241}$	Pb^{209}	Si^{32}	95.41	24.55	23.52	22.36	–	25.2	15.95	1.953×10^{-25}
$_{96}Cm^{241}$	Pb^{208}	Si^{33}	95.95	24.00	22.71	22.16	–	25.1	15.4	6.931×10^{-25}
$_{96}Cm^{241}$	Pb^{207}	Si^{34}	96.12	24.02	23.08	22.39	–	25.4	15.42	6.618×10^{-25}
$_{96}Cm^{242}$	Pb^{208}	Si^{34}	96.52	23.30	22.00	21.81	23.15	23.5	16.1	3.473×10^{-24}
$_{96}Cm^{243}$	Pb^{209}	Si^{34}	94.76	25.84	24.85	23.87	–	27.0	16.84	1.002×10^{-26}
$_{95}Am^{241}$	Hg^{206}	P^{35}	98.75	28.69	27.69	25.90	–	28.5	18.49	1.415×10^{-29}
$_{98}Cf^{249}$	Pb^{209}	S^{40}	110.20	29.52	27.55	26.63	–	–	–	2.093×10^{-30}
$_{98}Cf^{252}$	Hg^{206}	Ar^{46}	126.71	26.16	24.23	23.81	–	26.5	16.16	4.794×10^{-27}
$_{98}Cf^{249}$	Hg^{205}	Ar^{44}	124.29	29.80	28.27	26.36	–	–	–	1.098×10^{-30}
$_{98}Cf^{249}$	Hg^{204}	Ar^{45}	124.15	30.20	31.69	26.85	–	–	–	4.373×10^{-31}
$_{98}Cf^{250}$	Hg^{204}	Ar^{46}	125.59	28.12	29.56	25.35	–	28.2	19.52	5.257×10^{-29}
$_{98}Cf^{251}$	Hg^{206}	Ar^{45}	124.81	28.93	26.84	25.83	–	30.0	18.03	8.142×10^{-30}
$_{98}Cf^{251}$	Hg^{205}	Ar^{46}	126.15	27.14	25.70	24.58	–	28.6	16.24	5.020×10^{-28}
$_{99}Es^{252}$	Tl^{206}	Ar^{46}	129.28	25.24	23.89	23.01	–	27.5	17.64	3.988×10^{-26}
$_{99}Es^{253}$	Tl^{207}	Ar^{46}	129.77	24.37	22.40	22.32	–	25.5	18.17	2.956×10^{-25}
$_{99}Es^{254}$	Tl^{208}	Ar^{46}	128.47	26.12	24.72	23.67	–	28.2	17.72	5.257×10^{-27}
$_{99}Es^{254}$	Tl^{207}	Ar^{47}	128.94	25.60	23.70	23.43	–	27.9	17.2	1.741×10^{-26}
$_{99}Es^{253}$	Hg^{206}	K^{47}	135.66	25.80	23.69	22.99	–	26.3	19.6	1.098×10^{-26}
$_{99}Es^{254}$	Hg^{206}	K^{48}	135.07	26.62	24.60	23.80	–	–	18.22	1.662×10^{-27}
$_{101}Md^{255}$	Pb^{208}	K^{47}	142.30	21.98	19.47	19.86	–	–	29.80	4.373×10^{-33}
$_{101}Md^{258}$	Pb^{209}	K^{49}	139.63	25.49	23.17	22.87	–	–	–	3.897×10^{-26}
$_{98}Cf^{249}$	Pt^{200}	Ca^{49}	137.63	30.19	24.55	26.30	–	–	–	4.474×10^{-31}
$_{98}Cf^{250}$	Pt^{202}	Ca^{48}	137.69	29.41	30.82	25.94	–	28.5	18.81	2.696×10^{-30}
$_{98}Cf^{251}$	Pt^{201}	Ca^{50}	137.46	30.26	33.63	26.50	–	29.9	19.36	3.808×10^{-31}
$_{98}Cf^{252}$	Pt^{204}	Ca^{48}	138.78	27.96	25.26	24.32	–	–	19.96	7.599×10^{-29}
$_{99}Es^{252}$	Au^{204}	Ca^{48}	142.28	26.10	25.15	22.77	–	27.6	18.50	5.505×10^{-27}
$_{99}Es^{255}$	Au^{205}	Ca^{50}	142.64	25.26	22.73	22.48	–	26.5	17.66	3.808×10^{-26}
$_{101}Md^{254}$	Tl^{206}	Ca^{48}	150.06	21.12	19.64	18.72	–	23.2	17.22	5.257×10^{-22}
$_{101}Md^{255}$	Tl^{207}	Ca^{48}	150.09	20.91	18.81	18.55	–	21.6	18.73	5.137×10^{-22}
$_{101}Md^{257}$	Tl^{207}	Ca^{50}	149.60	21.29	19.17	19.25	–	22.3	17.59	3.554×10^{-22}
$_{101}Md^{258}$	Tl^{207}	Ca^{51}	148.62	22.57	20.81	20.39	–	25.7	20.89	1.415×10^{-27}
$_{102}No^{254}$	Pb^{206}	Ca^{48}	152.73	20.54	18.37	18.18	–	20.4	18.84	1.999×10^{-21}
$_{102}No^{255}$	Pb^{207}	Ca^{48}	153.53	19.27	17.17	17.23	–	20.8	16.47	3.722×10^{-20}
$_{102}No^{256}$	Pb^{208}	Ca^{48}	153.80	18.73	16.07	16.81	–	18.9	18.23	1.290×10^{-19}

The zero-point vibration energy

$$E_v = \frac{\pi}{2}\frac{\hbar\sqrt{2Q/\mu}}{(C_1 + C_2)}, \tag{10}$$

where μ is the reduced mass of the system and C_1 and C_2 are the 'central' radii of the fragments given by [14]

$$C_i = 1.18A_i^{1/3} - 0.48, \quad i = 1, 2. \tag{11}$$

The action integral K is given by $K = K_{\mathrm{L}} + K_{\mathrm{R}}$, where

$$K_{\mathrm{L}} = \frac{2}{h}\int_{r_a}^{r_t} [2B_r V(r)]^{1/2}\,\mathrm{d}r \tag{12}$$

$$K_{\mathrm{R}} = \frac{2}{h}\int_{r_t}^{r_b} [2B_r(r) V(r)]^{1/2}\,\mathrm{d}r. \tag{13}$$

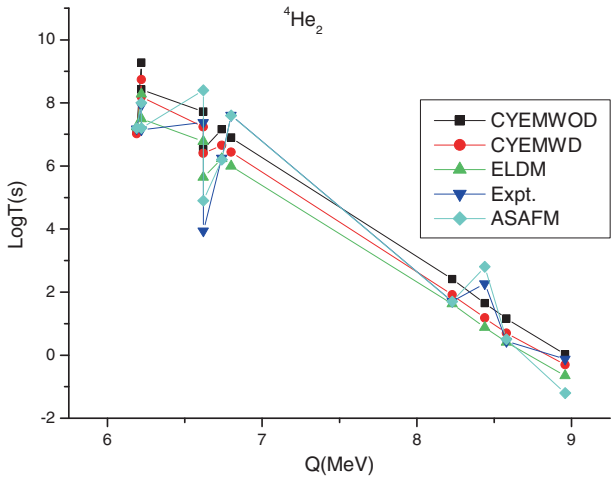

Figure 1. The comparison of computed α-decay half-life with the available values.

The limits of integration r_{a} and r_{b} are the two appropriate zeros of the integrand which are found numerically. Q-values for different decay modes are calculated using the experimental binding energies of Audi *et al* [15].

3. Results and discussion

In this work, all the possible modes of cluster radioactivity from neutron-rich parent nuclei in the actinide region have been investigated using CYEM model by including quadruple and hexadecapole deformations of the parent and daughter nuclei. The deformation parameter values are taken from ref. [16]. The calculated half-lives are in good agreement with the available data. Tables 1 and 2 give the logarithmic half-lives for α-decay and various clusters from neutron-rich parent nuclei with and without including deformation effects. From table 2, it is seen that the minimum half-lives are found for the decay leading to the doubly magic daughter nuclei ^{208}Pb for the cluster emission of ^{48}Ca from ^{256}No, ^{47}K from ^{253}Md and ^{32}Si from ^{240}Cm and near doubly magic daughter nuclei ^{207}Tl for the cluster emission of ^{34}Si from ^{241}Am, ^{46}Ar from ^{253}Es, ^{48}Ca from ^{255}Md respectively. Some of the nuclei have

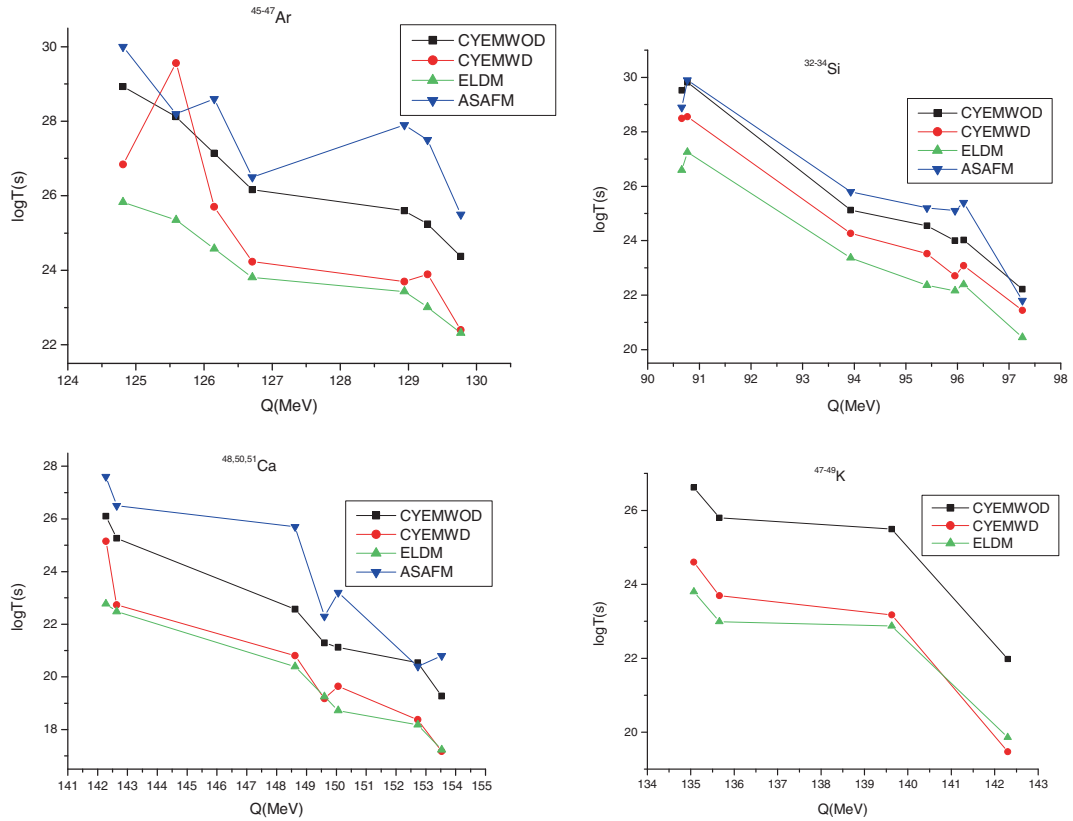

Figure 2. Plot for log T vs. Q values, of various clusters emitted from various parent nuclei.

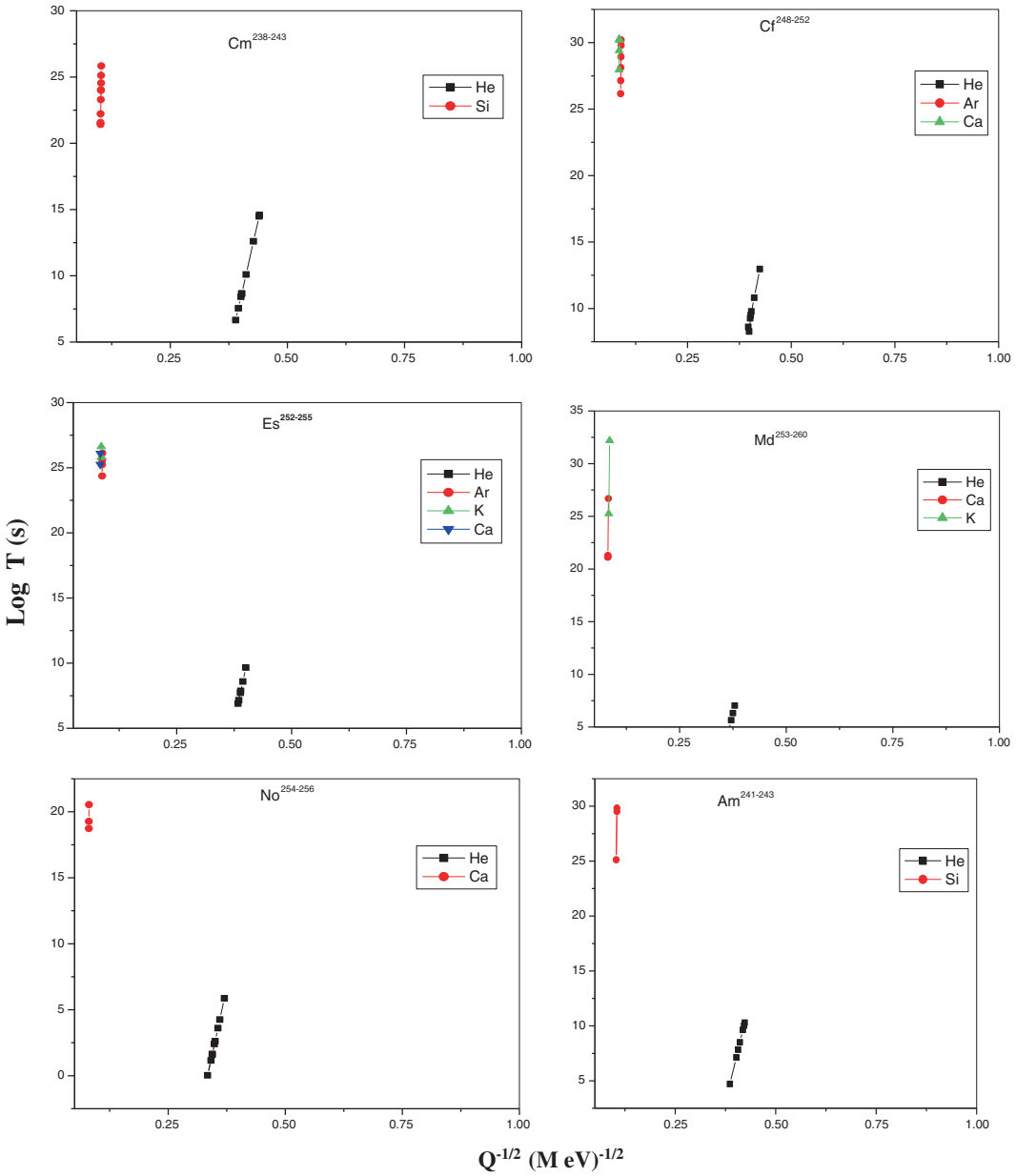

Figure 3. Geiger–Nuttal plots of some neutron-rich actinide nuclei for different cluster decays and α-decay.

longer half-lives indicating the stability and magicity of the corresponding parent nuclei. Figures 1 and 2 give the plot of logarithmic values of half-lives for α-decay and various clusters vs. Q values. The Geiger–Nuttal plots of some neutron-rich actinide nuclei for α-decay and various cluster emissions are shown in figure 3. Geiger–Nuttal plots for various clusters are found to be linear and most of the emitted clusters are α-like nuclei. Kumar *et al* [17] showed that α-like nuclei clusters are the most probable cases for measurements. Santhosh *et al* [18,19] have investigated the cluster decays on some trans-tin and trans-lead nuclei. Their results also show that α-like clusters have maximum cluster formation probability. Our results are in accord with theirs. Here we have presented the possible cluster decays which have $T<10^{30}$ s and the branching ratio relative to α-decay $\geq 10^{-18}$. The observed daughter nuclei are always doubly magic nuclei or their neighbouring nuclei. When deformation effects are included, half-life values are found to decrease slightly, because these effects reduce the height and width of the barrier. It is also found that neutron excess in the parent nuclei slows down the decay process, i.e. it increases the stability. The same result was obtained by our earlier work also [20]. Branching ratio relative to

α-decay, BR $= T_{\text{cluster}}/T_\alpha$, and decay constant, $\lambda = \ln 2/T_{1/2}$, are also calculated and included in the tabulation.

4. Conclusions

In this work, all the possible decay modes of cluster radioactivity from neutron-rich parent nuclei in the actinide region have been investigated using CYEM model. The calculated half-lives are in good agreement with the available theoretical values and experimental data. Here we have presented the possible cluster decay which have $T<10^{30}$ s and the branching ratio relative to α-decay $\geq 10^{-18}$. When deformation effects are included, half-life values are found to be decreased slightly, because deformation effects reduce the height and width of the barrier. It is also found that neutron excess in the parent nuclei slows down the decay process. With these we conclude that our results may be useful for future experiments.

References

[1] A Sandulescu, D N Poenaru and W Greiner, *Fiz. Elen. Chastits At. Yodra* **11**, 1334 (1980); *Sov. J. Part. Nucl.* **11**, 528 (1980)
[2] H J Rose and G A Jones, *Nature (London)* **307**, 245 (1984)
[3] R Blendowske, T Fliessbach and H Walliser, *Nucl. Phys. A* **464**, 75 (1987)
[4] S S Malik and R K Gupta, *Phys. Rev. C* **39**, 1992 (1989)
[5] B Buck and A C Merchant, *Phys. Rev. C* **38**, 450 (1985)
[6] Y J Shi and W J Swiatecki, *Nucl. Phys. A* **438**, 450 (1985)
[7] D N Poenaru, M Ivascu, A Sandulescu and W Greiner, *Phys. Rev. C* **32**, 572 (1985)
[8] K P Santhosh, R K Biju, S Sahadevan and A Joseph, *Phys. Scr.* **77**, 065210 (2008)
[9] R K Gupta, M Horoi, A Sandulescu, W Greiner and W Scheid, *J. Phys. G: Nucl. Part. Phys.* **19**, 2063 (1993)
[10] G A Pik-Pichak, *Sov. J. Nucl. Phys.* **44**, 923 (1986)
[11] Y J Shi and W J Swiatecki, *Nucl. Phys. A* **205**, 4649 (1987)
[12] G Shanmugam, G M Carmel Vigila Bai and B Kamalaharan, *Phys. Rev. C* **51**, 2616 (1995)
[13] H J Krappe, J R Nix and A J Sierk, *Phys. Rev. C* **20**, 992 (1979)
[14] R Hofstadeter, Nuclear radii, in: *Nuclear physics and technology* edited by H Schopper (Springer-Verlag, Berlin, 1967) Vol. 2
[15] G Audi, A H Wapstra and C Thivault, *Nucl. Phys. A* **729**, 337 (2003)
[16] P Moller, J R Nix, W D Myers and W J Swiatecki, *At. Data Nucl. Data Tables* **59**, 185 (1995)
[17] S Kumar, D Bir and R K Gupta, *Phys. Rev. C* **51**, 1762 (1995)
[18] K P Santhosh, R K Biju and S Sahadevan, *Nucl. Phys. A* **838**, 38 (2010)
[19] K P Santhosh and S Sahadevan, *Nucl. Phys. A* **847**, 42 (2010)
[20] G M Carmel Vigila Bai and S Santhosh Kumar, *DAE-BRNS Sym. Nucl. Phys. B* **45** (2002), a.67, p. 162
[21] S B Duarte, O A P Tavares, F Guzman and A Dimarco, *At. Data Nucl. Data Tables* **80**, 235 (2002)
[22] http://www.nndc.bnl.gov
[23] D N Poenaru, D Schnabel and W Greiner, *At. Data Nucl. Data Tables* **48**, 231 (1991)
[24] R Bonetti and A Guglielmetti, *Rom. Rep. Phys.* **59**, 301 (2007)